

## Identification of nucleolus-associated chromatin domains reveals the role of the nucleolus in the 3D organisation of the *A. thaliana* genome

Frédéric Pontvianne<sup>1,2,5,#</sup>, Marie-Christine Carpentier<sup>1,2</sup>, Nathalie Durut<sup>1,2</sup>, Veronika Pavlišťová<sup>3</sup>, Karin Jaške<sup>3</sup>, Šárka Šchořová<sup>3</sup>, Hugues Parrinello<sup>4</sup>, Marine Rohmer<sup>4</sup>, Craig S Pikaard<sup>5,6</sup>, Miloslava Fojtová<sup>3</sup>, Jiří Fajkus<sup>3,7</sup>, and Julio Saez-Vasquez<sup>1,2,7</sup>

<sup>1</sup>CNRS, Laboratoire Génome et Développement des Plantes, UMR5096, F-66860, Perpignan, France

<sup>2</sup>Université de Perpignan Via Domitia, Laboratoire Génome et Développement des Plantes, UMR5096, F-66860, Perpignan, France

<sup>3</sup>CEITEC-Central European Institute of Technology and Faculty of Science, Masaryk University, CZ-62500 Brno, Czech Republic

<sup>4</sup>Montpellier GenomiX, Montpellier Cedex 5, France

<sup>5</sup>Department of Biology and Department of Molecular and Cellular Biochemistry, Indiana University, Bloomington, IN 47405, USA

<sup>6</sup>Howard Hughes Medical Institute, Indiana University, Bloomington, IN 47405, USA

### Abstract

The nucleolus is the site of ribosomal RNA (rRNA) gene transcription, rRNA processing and ribosome biogenesis. However, the nucleolus also plays additional roles in the cell. We isolated nucleoli by Fluorescence Activated Cell Sorting (FACS) and identified Nucleolus-Associated Chromatin Domains (NADs) by deep sequencing, comparing wild-type plants and null mutants for the nucleolar protein, NUCLEOLIN 1 (NUC1). NADs are primarily genomic regions with heterochromatic signatures and include transposable elements (TEs), sub-telomeric regions and mostly inactive protein-coding genes. However, NADs also include active ribosomal RNA genes, and the entire short arm of chromosome 4 adjacent to them. In *nuc1* null mutants, which alter rRNA gene expression and overall nucleolar structure, NADs are altered, telomere association with the nucleolus is decreased and telomeres become shorter. Collectively, our studies reveal roles

---

<sup>#</sup>corresponding author: fpontvia@univ-perp.fr.

<sup>7</sup>co-senior authors

### ACCESSION NUMBERS

The NCBI accession number for the DNA-seq and RNA-seq data reported in this paper is SUB1340932 and BioProject ID is PRJNA312431.

### COMPETING INTERESTS

The authors (FP, MCC, ND, VP, KJ, SS, HP, MR, CSP, MF, JF, and JSV) declare no conflict of interest.

### AUTHOR CONTRIBUTIONS

MC performed most bioinformatic analyses. ND and VP realised telomere-shortening analyses of Figure 7. KJ, SS and MF realised and analysed the IP-TRAP assay of figure 7. HP and MR realised the deep sequencing. CSP, JF and JSV contributed to the design and/or the interpretation of the data. FP designed, performed and analysed all experiments except figure 7 and wrote the manuscript.

for NUC1 and the nucleolus in the spatial organization of chromosomes as well as telomere maintenance.

### Keywords

nucleolus; nuclear architecture; telomere; nucleolus-associated chromatin domains; heterochromatin

---

### Introduction

An important aspect of transcriptional regulation is the modification of gene accessibility to transcription factors and RNA polymerases. Gene accessibility depends on local chromatin structure but also on a gene's nuclear context and subnuclear localization. In recent years, local chromatin structure and its impact on gene expression has been extensively studied, with genome-wide approaches defining the chromatin contexts for each gene (Filion et al., 2010; Kharchenko et al., 2011; Roudier et al., 2011; Roy et al., 2010; Wang et al., 2008) and identifying chromatin states that correlate with gene activity (Bickmore and van Steensel, 2013; Sequeira-Mendes and Gutierrez, 2015). However, nuclear context is also important such that the position of a gene with respect to a nuclear pore, nuclear lamina or the nucleolus, as well as its inter or intra chromosome interactions with other loci, can affect its transcriptional regulation (Bickmore and van Steensel, 2013).

In mammalian cells, large portions of the genome associate with the network of nuclear lamina at the periphery of the nucleus and are identified as Lamina-Associated Domains (LADs). LADs are essentially composed of regions with silent chromatin signatures and can represent up to 35% of the nuclear genome (Guelen et al., 2008). Chromosome regions can also associate with the nucleolus, the largest nuclear body. The nucleolus forms as a direct consequence of ribosome biogenesis, but it is also implicated in stress sensing, cell cycle progression, viral replication and RNP biogenesis (Boisvert et al., 2007; Boulon et al., 2010; Pederson, 2011). Nucleolus-Associated Chromatin Domains (NADs) represent several megabases of the human genome from all 23 chromosomes, typically regions displaying silent chromatin signatures (Nemeth et al., 2010; van Koningsbruggen et al., 2010). Comparison of NADs and LADs has revealed substantial overlap. Interestingly, LADs that do not relocate to the nuclear periphery after mitosis often associate instead with the nucleolus (Kind et al., 2015, 2013). An important aspect of the nucleolus is that it creates a large domain within the nucleus from which RNA polymerase II (RNA pol II) is absent (Schubert and Weisshart, 2015). There is no membrane or physical barrier separating the nucleolus from the nucleoplasm, suggesting that nucleolar chromatin bears modifications that are refractive to Pol II transcription. Indeed, mutations in chromatin modifiers that localize and act (in part) in the nucleolus, such as Arabidopsis HISTONE DEACETYLASE 6, result in Pol II detection in the nucleolus as well as Pol II association with rRNA genes, which are normally transcribed only by Pol I (Earley et al., 2010). In plant cells neither LADs nor NADs have been identified so far. Importantly, plants lack genes orthologous to those encoding nuclear lamins in other eukaryotes. However, LINC (LITTLE NuCLEI, also called CRWN) proteins share some characteristics with lamins, including coiled-coil

domains (Dittmer et al., 2007). The composition of the LINC complex was recently characterized in plants (Graumann and Evans, 2011, 2010; Tatout et al., 2014). However, association between this complex and chromatin has not yet been demonstrated.

The relationship between rRNA gene transcription and organization and the nucleolus has been studied extensively (Benoit et al., 2013; Grummt and Langst, 2013; McStay and Grummt, 2008; Tucker et al., 2010). In each cell, active and inactive rRNA genes coexist and their ratio varies depending on the needs of the cell. Most silent copies of rRNA genes are excluded from the nucleolus, where RNA Polymerase I is located, but they relocate into the nucleolus in mutants that disrupt silencing (Pontvianne et al., 2013).

Ribosomal RNA genes are arranged in tandem arrays, (known as Nucleolus Organizer Regions, or NORs) that span millions of basepairs. Because silenced rRNA genes comprise a NOR on a different chromosome for active rRNA genes in *A. thaliana* (ecotype Col-0), changes in rRNA gene activity that are accompanied by changes in their subnuclear localisation are predicted to affect chromosome organization within the nucleus, at least locally. Using a technique that allows us to isolate nucleoli from plant tissue using FACS, combined with deep sequencing, we report here the identification of genomic NADs in the cell nuclei of *A. thaliana* leaves. We show here that NADs other than rRNA genes are mainly composed of transposable elements (TEs), but the NADs also contain genes that are mainly weakly expressed or unexpressed. Analyses of NADs in the *nucleolin 1* (*nuc1*) mutant, which disrupts rRNA gene silencing at the inactive NOR and alters nucleolar structure, reveals shows that NAD composition changes in *nuc1* versus wild-type nuclei. Interestingly, *nuc1* mutants also display shortened telomeres, and telomerase activity is detected in immunoprecipitated NUC1 fractions, revealing an unexpected role of the nucleolar protein, NUC1 in telomere maintenance.

## RESULTS

### 1. Identification of NADs in *A. thaliana*

DNA staining using the fluorescent dye, DAPI allows the visualization of nuclear DNA and its distribution within the nucleus. In nuclei of three-week-old *A. thaliana* leaves, bright DAPI-intensive signals correspond to chromocenters that include the highly compacted pericentromeric heterochromatin of the ten chromosomes. On the other hand, euchromatin is less compact and therefore the DAPI signal is less intense. DAPI staining of nuclei also allows one to identify the nucleolus, which appears as a black cavity in the nucleus due to a threefold lower concentration of DNA in the nucleolus compared to the surrounding nucleoplasm (excluding centromeres) (Figure 1A; see fluorescence intensity plot). To characterize this nucleolar DNA, we took advantage of a method that we recently developed for the purification of nucleoli by a modified Fluorescence-Activated Cell Sorting (FACS) approach. In this protocol, a nucleolar protein, Fibrillarin, is fused to yellow fluorescent protein (FIB2:YFP) and stably expressed in wild-type Col-0 plants to specifically mark nucleoli (Fig. 1A) (Pontvianne et al., 2013). Nucleoli liberated from sonicated nuclei are then isolated by Fluorescence-Activated Nucleolar Sorting (FANoS). Purified, sorted nucleoli stained by DAPI allow detection of nucleolar DNA (Figure 1B). As in the nucleoplasm, nucleolar DNA is not homogeneously distributed in the nucleolus and thus

stronger DAPI-stained signals are visible in some regions. Because the nucleolus forms around actively transcribed rRNA genes, rRNA genes are detected in nucleolar DNA, as expected, using DNA-Fluorescent *In Situ* Hybridization (FISH) and a probe flanking the transcription initiation site of rRNA genes (Figure 1B, see 45S rDNA signals). Interestingly, rDNA-FISH signals do not completely overlap with DAPI-stained nucleolar DNA, suggesting that nucleolar DNA does not consist solely of rRNA genes.

To determine the sequence of nucleolar DNA, two samples consisting of  $10^6$  nucleoli and two samples of  $5 \times 10^5$  nuclei from three week-old plants leaves were isolated. The nuclear or nucleolar DNA was then purified, sequenced and reads were mapped to the Arabidopsis TAIR10 reference genome. To identify genomic regions present in the nucleolus, we compared read densities of nuclear or nucleolar DNA for each of the two replicates. The nuclear fraction served as an input control to evaluate the relative enrichment of genomic regions in the nucleolar DNA. Genomic regions with a nucleolar versus nuclear (No/N) fold enrichment ratio greater than 2 in both replicates were considered nucleolus-associated chromatin domains (NADs) (Figure 1C). Excluding rRNA genes, NADs represent 4.2% of the genome (~5.7 Mb). Around 30% of NADs correspond to genes, 35% correspond to TEs and the rest correspond to intergenic regions (Figure 1D).

The No/N fold enrichment ratio was plotted along each of the five chromosomes in 100-kilobase windows to scan for genomic regions associated with the nucleolus (Figure 1E). In *A. thaliana*, 45S rRNA genes are arranged in tandem repeat arrays in NORs located on the left arms of chromosomes 2 and 4 (Figure 1E, *NOR2* and *NOR4*). In *A. thaliana* leaves only *NOR4* associates with the nucleolus and is actively transcribed, whereas *NOR2* is inactive and is excluded from the nucleolus (Chandrasekhara et al., 2016; Fransz et al., 2002; Pontvianne et al., 2013). This genomic configuration and selective expression of 45S rRNA genes is reflected in the enrichment of NADs along the left arm of chromosome 4 and the near absence from the left arm of chromosome 2 (Figure 1E). In fact, the entire left arm of chromosome 4 (or Chr4S for “Chromosome 4 short arm”), including its pericentromeric and centromeric regions, associates with the nucleolus (Figure 1E). In contrast, the left arm of chromosome 2 behaves like chromosomes 1, 3 and 5, which do not harbour NORs. Subtelomeric regions from all 5 chromosome pairs are also enriched in the nucleolus, consistent with previous work demonstrating telomere clustering at the periphery of the nucleolus (Armstrong et al., 2001).

## 2. NADs are enriched in inactive chromatin marks and TEs

We took advantage of published epigenomic data to characterize the types of chromatin that associate with NADs. Among the nine chromatin states defined based on their histone marks and histone variant content (Sequeira-Mendes et al., 2014), and presented in the Figure S1A, we found that four were statistically enriched in NADs (Figure 2A). This includes chromatin states 8 and 9, which show an enrichment for CG methylation, and for the silent chromatin marks, histone H3 lysine 9 dimethylation and histone H3 lysine 27 monomethylation (H3K9me2 and H3K27me1) (Sequeira-Mendes et al., 2014). Chromatin states 8 and 9 are typically associated with TEs and intergenic regions. In addition, chromatin states 4 and 5, which are characterized by high levels of H3 lysine 27 trimethylation (H3K27me3), are also

enriched in NADs. While almost no genes (other than TEs) are present in chromatin states 8 and 9, some are present in chromatin states 4 and 5. We therefore analysed the relative expression of polyA+ RNA from NAD-genes in these different chromatin states to establish a possible correlation between NADs and gene expression (Durut et al., 2014). All four of the chromatin states that are enriched in NADs (4, 5, 8 and 9) correspond to genomic regions depleted in actively transcribed genes (Figure 2B and Figure S1B) (Sequeira-Mendes et al., 2014).

Because NADs are enriched in TEs, we examined the relative contribution of each TE superfamily to NADs. 3640 TEs were identified with a No/N fold enrichment ratio greater than 2 (NAD-TEs; Supplemental data 1). In general, no TE superfamily is particularly enriched (Figure 2C). *DNA/Mariner*, *DNA/Pogo*, *DNA/Tc1* and *pseudo-LINE* elements are slightly overrepresented, while *LTR/Copia* or *SINE* superfamilies are underrepresented. The biased presence of particular TE superfamilies in NADs is probably a consequence of their relative abundance in peri-centromeric or knob regions (Figure 2D).

### 3. Description of the genes present in NADs

Although a large portion of NAD loci correspond to TEs, there are also many genes. Using the Araport11 annotation database, and excluding 317 Araport11-referenced TEs and rRNA genes, a total of 907 genes were identified as NAD-genes, which represent around 3% of all genes (Supplemental data 2). The relative position of NAD-genes along all five chromosomes follows the general distribution of NADs, being enriched in subtelomeric regions and in the short arm of chromosome 4 (Figure 3A). NAD-gene distribution among Eukaryotic orthologous groups of proteins (KOG) revealed that most types of KOGs are represented among NAD-genes, with only a slight enrichment for the “cell mobility” category. However, only 21 genes belong to this particular category and the 4.7% proportion observed here is only due to the association of 1 gene and is therefore not considered significant. Genes implicated in “translation, ribosomal structure and biogenesis”, and which are thus linked to nucleolar function, are not enriched among NAD-genes either. However, two other categories of genes are particularly enriched: pseudogenes and tRNA genes (Figure 3B). Among the 915 pseudogenes referenced in the *A. thaliana* genome, 72 (7.9%) are present in NAD-genes. Moreover, 7.2% of tRNA genes belong to NADs. Interestingly, almost all tRNA isoacceptor types are present in NADs, with the exception of tRNA-His which is the smallest tRNA gene family in *A. thaliana* (Figure 3D). The global distribution of pre-tRNA genes among the ten chromosome arms shows that 31% are clustered on the short arm of chromosome 2 (Figure S2). Because RNA Pol II is not observed in the nucleolus, we expected that predicted Pol II-transcribed genes that are among NAD-genes would likely be unexpressed or expressed at low levels. Global nuclear gene and NAD-gene expression analyses did indeed reveal a bias in expression that supports this hypothesis (Figure 3C).

### 4. Impact of NOR positioning and nucleolus structure on NAD composition

In wild-type *A. thaliana* leaves, only *NOR4* interacts with the nucleolus while *NOR2*, composed of inactive rRNA genes, is excluded from the nucleolar periphery. In null mutants for the *NUCLEOLIN 1* gene (*nuc1*), *NOR2* and *NOR4* both associate with the nucleolus and

the *NOR2* rRNA genes that are normally silenced during development in wild-type leaves fail to silence (Earley et al., 2010; Pontvianne et al., 2010). *VAR1* designates a class of rRNA genes that represent 50% of the entire set of rRNA genes. Because *VAR1* rRNA genes are present at the inactive *NOR2* they are excluded from the nucleolus, which explains the lack of *VAR1* gene expression in wild-type Col-0 (Chandrasekhara et al., 2016; Pontvianne et al., 2010). However, we previously demonstrated that *VAR1* rRNA genes are expressed in *nuc1* mutants (Pontvianne et al., 2010). Here, we show using PCR analyses of FACS-isolated nuclear or nucleolar DNA that *VAR1* rRNA genes indeed associate with the nucleolus in the *nuc1* mutant (Figure 4A). To test the impact of *NOR2* association with the nucleolus on NAD composition, we isolated and sequenced the DNA from FACS-isolated nuclei or nucleoli of *nuc1*. In wild-type Col-0, chromosome 4 harbours the largest proportion of NADs due to the association of Chr4S with the nucleolus, followed by chromosome 2 (Figure 1). However, in *nuc1*, the short arms of both chromosomes 2 and 4 (Chr2S and Chr4S) associate with the nucleolus (Figure 4B). This observation correlates with the transcriptionally active state of both *NOR2* and *NOR4* in *nuc1* (Figure 4A).

The pericentromeric and centromeric regions of chromosomes 1, 3 and 5 become enriched in *nuc1* mutant NADs (Figure 4C and Figure S3). However Interestingly Modullo, the nucleolin homolog in *Drosophila melanogaster*, is required for centromere sequestration at the periphery of the nucleolus (Padeken et al., 2013), such that centromere association with Arabidopsis nucleoli might be expected to decrease rather than increase in *nuc1* mutants. Because centromeric chromocenters are easily detected by DAPI staining, we assessed their relative positions with respect to the nucleolus in wild-type Col-0 and in *nuc1* mutant nuclei from three-week-old leaves (Figure 4D). In addition, an immunolocalisation approach with an antibody recognizing the centromeric Histone 3 (cenH3) were used here to validate the nuclear centromeres distribution. Consistent with the NAD analyses, centromeres associate more strongly with the nucleolus in *nuc1* relative to wild-type (p-value < 2.2e-16) (Figure 4D). In 16% of the nuclei, a strong DAPI-stained signal can be detected inside Col-0 nucleoli; by contrast, more than 72% of *nuc1* nucleoli harbour these heterochromatin signatures (p-value < 2.2e-16) (Figure 4D). The altered centromere positioning in *nuc1* mutant nuclei suggests, as in *D. melanogaster*, a role for NUC1 in heterochromatin distribution, but in an opposite way.

## 5. NAD-gene depletion in the *nuc1* mutant

822 NAD-TEs (Supplemental data 3) and 117 NAD-genes (Supplemental data 4) can be identified in *nuc1* with a No/N fold enrichment ratio greater than 2. Their distribution along the five chromosomes (Figure 5A) is quite different from that seen in wild-type Col-0 (see Figure 3A). While 65% of Col-0 NAD-genes were distributed on chromosome 4, only 20% of *nuc1* NAD-genes are present on this chromosome. By contrast, 13% of Col-0 NAD-genes were found on chromosome 2, but this proportion increased to 46% in the *nuc1* mutant. Nonetheless, the NAD-gene pool between wild-type Col-0 and *nuc1* overlaps significantly, since 80% of *nuc1* NAD-genes are also NAD-genes in Col-0 (Figure 5B). To further characterize NAD-genes that strongly associate with the nucleolus, we identified NAD-genes in either wild-type Col-0 or *nuc1* that have a No/N fold enrichment ratio greater than 3 (Figure 5C). In both cases about 100 NAD-genes were identified, and 51 were shared in both

genotypes. Among these common loci are tRNA genes (8) and pseudogenes (21), demonstrating their strong, reproducible association with the nucleolus, even in the *nuc1* mutant context where nucleolar structure is disrupted (Pontvianne et al., 2007).

Because RNA pol II is generally not detected in the nucleolus, we hypothesized that the physical association of NAD-genes with the nucleolus may reflect their transcriptional status. We thus took advantage of the fact that several hundred NAD-genes detected in wild-type no longer associate with the nucleolus in the *nuc1* mutant to see if loss of nucleolar localization correlates with their activity. RNA deep sequencing analyses of Col-0 versus the *nuc1* mutant from three-week-old leaves were performed in triplicate, allowing us to identify 100 up-regulated genes in the *nuc1* mutant (Figure 5C). Among these 100 up-regulated genes, 4 are NAD-genes in wild-type but not in the *nuc1* mutant. Three of these 4 genes, which are all on chromosome 4, are shown in Figure 5D–F; they encode for a P-loop nucleoside triphosphate hydrolase (AT4G05380), a WRKY transcription factor (AT4G01720) and a pseudogene (AT4G08093), respectively. Note that only genes considered up-regulated in *nuc1* by software CUFFDIFF were taken into consideration here. However, more transcripts can be detected in the same region of Chr4S where nucleolar association in *nuc1* is weaker than in wild-type (Figure S4). These observations reinforce a possible link between gene activity and nucleolus association.

## 6. Nucleolar clustering of telomeres is disrupted in the *nuc1* mutant

In *nuc1* mutants, nucleolar organization is disrupted (Pontvianne et al., 2007). Because previous studies have shown that Arabidopsis telomeres cluster at the periphery of the nucleolus (Armstrong et al., 2001; Franz et al., 2002), nucleolar disruption in *nuc1* might alter telomere positioning, potentially influencing the association of linked chromosomal loci with the nucleolus. In the global distribution of NADs along all five chromosomes (Figure 1E), a convex pattern is observed, meaning that sub-telomeric regions are largely enriched in the nucleolus. Interestingly, the sub-telomeric nucleolar association is lower in the *nuc1* mutant compared to wild-type Col-0, especially for chromosomes 1, 3 and 5 (Figure 4B). This observation is confirmed by the analysis of the relative enrichment in the nucleolus of genomic regions in the *nuc1* mutant compared to wild-type Col-0 (Figure 6A). The latter distribution pattern is concave, demonstrating the enrichment of the centromeric and pericentromeric regions as NADs, but also the depletion of sub-telomeric regions, in the *nuc1* mutant.

The deep sequencing data strongly suggest that nucleolar clustering of telomeres is affected in the *nuc1* mutant. To test this hypothesis with a different method, we conducted DNA Fluorescent In Situ Hybridization (FISH) analyses of the telomere distribution in wild-type Col-0 and *nuc1* leaf nuclei by using telomere-specific probes (Figure 6 B–D and Figure S5). As expected, FISH signals tend to associate with the nucleolus in wild-type Col-0 nuclei (Figure 6B). However, a significant decrease in telomere association with the nucleolus is observed in the *nuc1* mutant (Figure 6C), with quantification revealing an 83% telomere-nucleolus association in wild-type Col-0 versus 53% in the *nuc1* mutant (Figure 6D). Importantly, telomeres that do not associate with the nucleolus in *nuc1* do not appear to cluster in an alternative nucleoplasmic subcompartment.

## 7. Mutations in *NUC1* cause telomere shortening on all chromosome arms

The biological function of telomere nucleolar clustering remains unknown, but we reasoned that it could have an impact on telomere maintenance. The analysis of terminal chromosome restriction fragments (TRF) allows one to determine global telomere size. We used this technique to determine telomere size distributions in wild-type Col-0 and *nuc1* mutants. In addition, telomere size was analysed in a mutant for the *NUC2* gene, which encodes another nucleolin-like protein whose function differs from NUC1 (Durut et al., 2014). In addition, telomere size was analysed in mutants for genes encoding FASCIATA1 (*fas1-4*) and FASCIATA2 (*fas2-4*), which mediate replication-dependant histone deposition and whose disruption strongly reduces telomere size (Mozgova et al., 2010). Compared to wild-type Col-0, a significant TRF length reduction was observed in both *nuc1* mutant alleles, comparable to that observed in *fas1* and *fas2* mutants (Figure 7A). However, no difference is observed between wild-type Col-0, the *nuc2* mutant or the complemented *nuc2* mutant, demonstrating the specific effect of the *nuc1* mutations.

We demonstrated previously the importance of NUC1 on rRNA gene regulation, which occurs in *NOR2* and *NOR4* (Pontvianne et al., 2010, 2007). In *A. thaliana*, the terminal rRNA genes from *NOR2* and *NOR4* are directly capped by telomere repeats (Copenhaver and Pikaard, 1996). To determine if telomeres of NOR-bearing-chromosomes are differentially affected, we used a PCR-based method called PETRA (primer extension telomere repeat amplification) (Heacock et al., 2004) on multiple chromosome arms (Figure 7B–E). In agreement with the data from TRF, telomeres on all studied chromosome arms display a ~30% loss of length in the *nuc1* mutants compared to wild-type Col-0, which is equivalent to the loss observed in *fas1* and *fas2* mutants. Together, these observations demonstrate that telomeres from all chromosome arms are shortened in *nuc1* and thus is not dependent on the presence of rRNA genes near the affected telomere.

The fact that telomeres tend to associate less frequently with the nucleolus and are shorter in *nuc1* mutants compared to wild-type indicates that NUC1 is somehow important for telomere biology. Whether these effects are due to the *NUC1* disruption, nucleolus disorganisation or both remain unknown. To test whether NUC1 interacts directly or indirectly with the telomerase, a Telomere Repeat Amplification Protocol (TRAP) was performed using immunoprecipitated NUC1 (Figure 7F). IP was performed using an anti-FLAG antibody and protein extracts of WT Col-0 or *nuc1* mutant complemented with a transgene encoding NUC1 fused to a Flag epitope tag under the control of its own promoter (NUC1-Flag) (Pontvianne et al., 2010). Telomerase activity is markedly stronger in the NUC1-FLAG co-IP sample (FLAP-IP, left panel), compare to the background signal observed in the Col-0 plant. These data suggest that NUC1 interacts with and co-IPs telomerase activity, suggesting a direct role in NUC1 telomere biology.

## DISCUSSION

### The impact of NOR-nucleolus associations on nuclear architecture

In mammalian cells the nuclear distribution of DNA is governed by individual chromosome territories (Gibcus and Dekker, 2013). Although chromosome territories can be seen in *A.*



*thaliana* cells, their distribution in the nucleus is stochastic, with the exception of NOR-bearing-chromosomes 2 and 4 (Pecinka et al., 2004). *NOR4*, composed of rRNA gene variants *VAR2* and *VAR3*, associates with the nucleolus (Pontvianne et al., 2013). We demonstrate here that *NOR4* and the entirety of Chr4S, including centromeric and pericentromeric regions, associates with the nucleolus. Consequently, this entire region represents a specific territory or subnuclear compartment. Interestingly, data obtained by chromosome conformation capture indicates that this region acts as an interaction insulator (Feng et al., 2014; Grob et al., 2013). Our results suggest that nucleolus association may be the basis for this insulation.

Coincident with *NOR2* rRNA gene expression in certain mutant backgrounds, the *NOR2* genomic region becomes associated with the nucleolus. Failure to silence *NOR2* rRNA genes occurs in mutants for genes encoding factors implicated in rRNA genes dosage control, such as mutants for histone modifiers (Earley et al., 2010; Pontvianne et al., 2012) as well as *nuc1* (Pontvianne et al., 2010, 2007). As observed for *NOR4* in wild-type Col-0, *NOR2* rRNA gene expression correlates with its nucleolar association, but also the nucleolar association of Chr2S, including its centromeric and pericentromeric region. Whether *NOR2* rRNA genes nucleolar association lead to this change in the nuclear organisation or whether NUC1 influences this organization remain to be tested.

Although Chr4S and/or Chr2S associate with the nucleolus under certain conditions, not all genes present in these genomic regions are necessarily associated with the nucleolus. Loops emanating from Chr4S and oriented within the interior of the nucleus probably exist, allowing actively expressed genes to access a nearby nuclear environment compatible with active gene expression, as previously described (Feng et al., 2014; Fransz et al., 2002).

### Pol II transcribed genes are present in NADs

Our data have allowed the comprehensive identification of genetic loci that associate with the nucleolus (NADs), including many genes (NAD-genes). The majority of NADs correspond to repeat elements such as TEs that are transcriptionally silenced by repressive histone modifications and DNA methylation (Ito and Kakutani, 2014). Whether the association of these loci with the nucleolus participates in transcriptional repression is an open question. However, because only a fraction of TEs associate with the nucleolus, being in a NAD is certainly not a prerequisite for silencing. Our data also demonstrate the presence of genes other than in TEs in NADs. In the human nucleolus-associated genome, genes encoding for olfactory receptors or transcription factors were found to be enriched in NAD-genes (Nemeth et al., 2010; van Koningsbruggen et al., 2010). In our data, the most enriched non-rRNA gene loci are pseudogenes. Because they potentially encode truncated or non-functional proteins, keeping them silent is perhaps the best way to prevent a potential deleterious effect of their expression. Importantly, pseudogenes remain highly enriched in the nucleolus of *nuc1* mutant cells, although its structure is greatly disrupted (Figure 5).

Genes encoding pre-tRNAs are also significantly enriched in the nucleolus. Although this association has never been described in plant cells, previous reports showed a nucleolar association of tRNA genes in yeast and human cells (Nemeth et al., 2010; Thompson et al., 2003). Interestingly, the presence of a nearby tRNA gene was shown to antagonize Pol II

RNA transcription in yeast, due to its clustering near or in the nucleolus (Wang et al., 2005). This phenomenon is known as tRNA gene-mediated silencing and involves the proteins MOD5 and Condensin (Haeusler et al., 2008; Pratt-Hyatt et al., 2013). However, we show here that several hundred functional genes associate with NADs and only a small portion have a tRNA gene nearby. Other mechanisms to explain tRNA gene nucleolar association may exist. Whether their association with the nucleolus is biologically relevant remains unknown, but because RNA Pol II is depleted in the nucleolus, sequestration of genes to NADs likely reflects a chromatin status or location not conducive to Pol II transcription. This hypothesis is reinforced by the observation that NAD-genes are typically silent or expressed at low levels, but also by the fact that some genes that were NAD-genes in Col-0, but not in *nuc1*, became significantly up-regulated in *nuc1* (Figure 5). These observations reinforce a possible link between gene silencing and nucleolus association.

Regulation by nucleolar sequestration is known to control certain protein functions, especially during stress conditions. In mammalian cells rDNA intergenic transcripts accumulate in the nucleolus after heat shock and provoke the nucleolar sequestration of nuclear proteins like the DNA methyltransferase DNMT1, the proteasome factor SUG1, or POLD1, a key factor of DNA replication (Audas et al., 2012a, 2012b). A similar mechanism may exist to regulate transcription by a phenomenon that could be named transcriptional regulation by nucleolar sequestration.

### **Telomere maintenance and/or protection require their physical association with the nucleolus**

In *A. thaliana*, telomeres tend to associate with the nucleolus (Armstrong et al., 2001; Franz et al., 2002; Roberts et al., 2009). Consequently, we expect subtelomeric regions to be near the nucleolus, as shown previously by DNA-FISH (Schubert et al., 2012). Our data demonstrate that at least 100 kb of each region flanking the telomeres strongly associates with the nucleolus. This association may have an impact on genes present in these regions. 39% of highly enriched NAD-genes in Col-0 (No/N > 3) are distributed in these subtelomeric regions, while they represent less than 1% of the genome. The biological function of telomere nucleolar clustering remains unknown, but some studies have indicated a link between telomere biology and the nucleolus (reviewed in (Dvorackova et al., 2015; Pederson, 1998; Schubert et al., 2014)). In human cells, the telomerase reverse transcriptase (TERT), which catalyses reverse transcription of the telomerase RNA template into telomeric repeats, is activated in the nucleolus during S phase (Jady et al., 2006; Lee et al., 2014; Tomlinson et al., 2006). In *A. thaliana* a preferential nucleolar accumulation of telomere repeat binding (TRB) MYB-like proteins was shown (Dvorackova et al., 2010). In addition, the telomerase RNA-binding protein dyskerin, AtNAP57/CBF5, and AtTERT accumulate in the plant nucleolus (Kannan et al., 2008; Lermontova et al., 2007).

NADs identification in the *nuc1* mutant revealed a decrease of telomere-nucleolus association. In the same time, we demonstrate that telomeres are shortened in the *nuc1* mutant. Previous work demonstrated the important role of nucleolin in rRNA organization and biogenesis (reviewed in (Durut and Saez-Vasquez, 2015)). However, all telomeres are affected in *nuc1*, so the proximity of rRNA genes on NOR-bearing chromosome cannot

explain telomere shortening. Subnucleolar structures show profound changes in *nuc1* mutants, such as the loss of fibrillar centers (FC), reductions in the dense fibrillar component (DFC), as well as an alteration of the granular component (GC) (Pontvianne et al., 2007). FC, DFC and GC are subnucleolar structures that are conserved in most eukaryotes and that reflect various steps of ribosome biogenesis (reviewed in (Stepinski, 2014; Thiry and Lafontaine, 2005)). The nucleolar disorganization observed in *nuc1* mutants reflects the impact of these mutations on rRNA gene regulation. But *nuc1* mutants also affect non-ribosomal nucleolar functions. Co-IP TRAP experiments indeed argue in favour of a direct role of NUC1 in telomere biology. Whether NUC1 interacts directly or indirectly with the telomerase holoenzyme will have to be demonstrated by further experiments. In addition, we cannot conclude whether telomere shortening is a cause or a consequence of telomere mislocalisation. However, telomere clustering is not specific to *A. thaliana*. In budding yeast, telomeres cluster in foci at the nuclear periphery in cycling cells (Meister and Taddei, 2013). In quiescent cells, a lack of carbon source is followed by telomeres clustering into a unique focus, in the centre of the nucleus (Guidi et al., 2015). Although we do not have direct evidence to show it, these data argue in favour of a model where telomere shortening is a consequence of telomere mislocalisation, probably due to the absence of NUC1. Combined with previous studies, our work strongly suggests a role for the nucleolus in the biology of telomeres.

## MATERIAL AND METHODS

### Plant materials and growth conditions

Seeds corresponding to *nuc1-1* and *nuc1-2* (referenced as *nuc1* through the manuscript) plants lines (SALK\_053590 and SALK\_002764 respectively) were previously reported in (Pontvianne et al., 2010, 2007) and are available through the Nottingham Arabidopsis Stock Centre (NASC). Seeds of *nuc2-2* mutant (SALK GABI\_178D01) and *nuc2:NUC2* complemented line were described in (Durut et al., 2014). Third generation of the knockout mutant *fas1-4* (SAIL\_662\_D10) and *fas2-4* (SALK\_033228) are used in figure 7 and were described in (Exner et al., 2006). For FANoS, wild-type Col-0 expressing the FIB2:YFP fusion protein was described in (Pontvianne et al., 2013). The *nuc1-2* plants were crossed with Col-0 FIB2:YFP to introgress the nucleolar marker in the *nuc1-2* mutant background. All plant material used here were grown in control growth chambers, on soil at 21°C with a day light period of 16h per day.

### Nuclear and Nucleolar DNA preparation and sequencing

1 gram of leaves from 3-week-old FIB2:YFP plants are fixed for 20 min in 4% formaldehyde in Tris buffer (10 mM Tris-HCl at pH 7.5, 10 mM EDTA, 100 mM NaCl) and are then washed twice for 10 min in ice-cold Tris buffer. Washed leaves are minced with a razor blade in 1 mL of 45 mM MgCl<sub>2</sub>, 20 mM MOPS (pH 7.0), 30 mM sodium citrate, and 0.1% Triton X-100. The homogenate is filtered through 30µm mesh (PARTEC CellTrics) and subjected to FACS to sort nuclei or sonicated using a Bioruptor (three 5-min pulses, medium power; Diagenode) to liberate nucleoli that were then sorted by FANoS. Sorting of nuclei or nucleoli was triggered by the FIB2:YFP signal using a BD FACS Aria II. Sorted nuclei or nucleoli were treated with RNase A and proteinase K prior to purification and

concentration using the kit ChIP DNA Clean & Concentrator (Zymo Research). DNA libraries were generated via the kit Nextera XT DNA sample preparation (Illumina®) according to manufacturer's instruction, and were then subjected to high throughput paired-end 2X125nt sequencing on a HiSeq 2500 apparatus (Illumina®). Around 40 million clusters were recovered from the sequencing for each sample.

### Cytogenetic Analyses

DNA-FISH and or DAPI-stained nuclei analyses were performed using nuclei from leaves of 3 or 4-week-old plants as described previously in (Pontvianne et al., 2012). The 45S rRNA gene probe was generated by PCR on total genomic DNA from Col-0 wild-type and correspond to the region flanking the 45S rRNA genes transcription initiation site (from -223 to +243). Telomere-specific probe was generated by PCR on total genomic DNA from Col-0 wild-type with the primer 5Telo (TTTAGGGTTTAGGGTTTAGGGTTTAGGGTTTAGGG) and 3Telo (CCCTAAACCCTAAACCCTAAACCCTAAACCCTAAA) prior to its labelling with digoxigenin-11-UTP (Roche). Immunolocalisation experiments were performed as previously describe in (Durut et al., 2014), using the antibody anti-cenH3 (HTR12 NBP1-18694, Novus Biologicals).

### Evaluation of telomere lengths using TRF and PETRA analysis

Nucleon Phytopure Genomic DNA Extraction Kits (Illustra) were used for DNA extraction according to manufacturer's protocol from 3 week-old rosette leaves. Five hundred ng of genomic DNA were analysed either by terminal restriction fragment analysis (TRF) or by method of primer extension telomere repeat amplification (PETRA). TRF analysis was performed according to (Ruckova et al., 2008) and samples were digested by MseI (NEB). For PETRA method (Vespa et al., 2007) chromosome specific primers for 3L, 4R, 5L and 5R described in (Heacock et al., 2004) were used. Samples from both types of analysis were then separated by 0,8% agarose gel electrophoresis followed by Southern hybridization with [<sup>32</sup>P]-labelled telomeric probe TR4C (CCCTAAA)<sub>4</sub>.

### IP-TRAP (Immunoprecipitation-Telomere Repeat Amplification Protocol)

For IP-TRAP, see Supplemental informations.

### Bioinformatic and statistical analyses

For each library, 30–50 · 10<sup>6</sup> reads were obtained with 85–90% of the bases displaying a Q-score > 30, with a mean Q-score of 38 as assessed with Fastqc. After, filtering out of reads corresponding to chloroplastic, mitochondrial and rRNA genes was performed with Bowtie 2 (Langmead and Salzberg, 2012). Remaining reads were mapped against the TAIR 10\_genome with bowtie2 in sensitive local mode and no mismatch. TEs were analysed according to the annotation published in (Flutre et al., 2011). Quantification by 100kb windows was made with bedtools software (<http://bedtools.readthedocs.org/en/latest/>). Regions with a fold-change No/N superior to 2 are tagged differentially covered (DC). The data are presented in the supplemental data 5.

Total RNA was extracted from three pools of three week-old Arabidopsis plant leaf tissues of wilt-type Col-0 or *nuc1* mutant using TRIzol reagent (MRC, Inc.). Sequencing was performed by the MGX facility (Montpellier) using a Hiseq 2000 to generate 1X 51bp long reads. Illumina reads from non-stranded, polyA+ RNA deep sequencing libraries were aligned to the *A. thaliana* TAIR10 annotated genome reference using Tophat2, Cufflinks, Cuffmerge and Cuffdiff (Langmead and Salzberg, 2012).

The Z test calculation for 2 Population Proportions was used to whether or not the data differ between wild-type Col-0 and *nuc1* mutant in figures 2A, 3D, 4E and 6D.

## Supplementary Material

Refer to Web version on PubMed Central for supplementary material.

## Acknowledgments

The authors are grateful to Eric Lasserre for his help in TEs analyses, Pascale Comella for her logistic support, Claire Picart for her help in confocal microscopy, Todd Blevins for correcting English and Marie Mirouze for fruitful discussions. We also thank the flow cytometry facility of Montpellier RIO Imaging. This work was supported by CNRS, ANR JCJC NucleoReg (ANR-15-CE12-0013-01) and by BQR2014 (UPVD) LANoS to FP, ANR SubCellif (SVSE2\_SUBCELIF 087217) to JS and GA R 16-01137S to JF. The international collaboration between France and the Czech republic is supported by the Barrande program to JS (35626NL) and JF (7AMB16FR014). This work was initially supported by the National Institutes of Health (USA) grant GM60380 to CSP, who is an Investigator of the Howard Hughes Medical Institute and the Gordon and Betty Moore Foundation. The international collaboration between the laboratory of CSP and JF is funded by “ the Ministry of Education, Youth and Sports of the Czech Republic under the project CEITEC 2020 (LQ1601) and KONTAKT II (LH15189).”

## References

- Armstrong SJ, Franklin FC, Jones GH. Nucleolus-associated telomere clustering and pairing precede meiotic chromosome synapsis in Arabidopsis thaliana. *J Cell Sci.* 2001; 114:4207–4217. [PubMed: 11739653]
- Audas TE, Jacob MD, Lee S. The nucleolar detention pathway: A cellular strategy for regulating molecular networks. *Cell Cycle Georget Tex.* 2012a; 11:2059–2062. DOI: 10.4161/cc.20140
- Audas TE, Jacob MD, Lee S. Immobilization of proteins in the nucleolus by ribosomal intergenic spacer noncoding RNA. *Mol Cell.* 2012b; 45:147–157. DOI: 10.1016/j.molcel.2011.12.012 [PubMed: 22284675]
- Benoit M, Layat E, Tourmente S, Probst AV. Heterochromatin dynamics during developmental transitions in Arabidopsis - a focus on ribosomal DNA loci. *Gene.* 2013; 526:39–45. DOI: 10.1016/j.gene.2013.01.060 [PubMed: 23410919]
- Bickmore WA, van Steensel B. Genome architecture: domain organization of interphase chromosomes. *Cell.* 2013; 152:1270–1284. DOI: 10.1016/j.cell.2013.02.001 [PubMed: 23498936]
- Boisvert FM, van Koningsbruggen S, Navascues J, Lamond AI. The multifunctional nucleolus. *Nat Rev Mol Cell Biol.* 2007; 8:574–585. DOI: 10.1038/nrm2184 [PubMed: 17519961]
- Boulon S, Westman BJ, Hutten S, Boisvert FM, Lamond AI. The nucleolus under stress. *Mol Cell.* 2010; 40:216–227. DOI: 10.1016/j.molcel.2010.09.024 [PubMed: 20965417]
- Chandrasekhara C, Mohannath G, Blevins T, Pontvianne F, Pikaard CS. Chromosome-specific NOR inactivation explains selective rRNA gene silencing and dosage control in Arabidopsis. *Genes Dev.* 2016; 30:177–190. DOI: 10.1101/gad.273755.115 [PubMed: 26744421]
- Copenhaver GP, Pikaard CS. RFLP and physical mapping with an rDNA-specific endonuclease reveals that nucleolus organizer regions of Arabidopsis thaliana adjoin the telomeres on chromosomes 2 and 4. *Plant J Cell Mol Biol.* 1996; 9:259–272.

- Dittmer TA, Stacey NJ, Sugimoto-Shirasu K, Richards EJ. LITTLE NUCLEI genes affecting nuclear morphology in *Arabidopsis thaliana*. *Plant Cell*. 2007; 19:2793–2803. DOI: 10.1105/tpc.107.053231 [PubMed: 17873096]
- Durut N, Abou-Ellail M, Pontvianne F, Das S, Kojima H, Ukai S, de Bures A, Comella P, Nidelet S, Rialle S, Merret R, Echeverria M, Bouvet P, Nakamura K, Saez-Vasquez J. A duplicated NUCLEOLIN gene with antagonistic activity is required for chromatin organization of silent 45S rDNA in *Arabidopsis*. *Plant Cell*. 2014; 26:1330–1344. DOI: 10.1105/tpc.114.123893 [PubMed: 24668745]
- Durut N, Saez-Vasquez J. Nucleolin: dual roles in rDNA chromatin transcription. *Gene*. 2015; 556:7–12. DOI: 10.1016/j.gene.2014.09.023 [PubMed: 25225127]
- Dvorackova M, Fojtova M, Fajkus J. Chromatin dynamics of plant telomeres and ribosomal genes. *Plant J Cell Mol Biol*. 2015; 83:18–37. DOI: 10.1111/tpj.12822
- Dvorackova M, Rossignol P, Shaw PJ, Koroleva OA, Doonan JH, Fajkus J. AtTRB1, a telomeric DNA-binding protein from *Arabidopsis*, is concentrated in the nucleolus and shows highly dynamic association with chromatin. *Plant J Cell Mol Biol*. 2010; 61:637–649. DOI: 10.1111/j.1365-313X.2009.04094.x
- Earley KW, Pontvianne F, Wierzbicki AT, Blevins T, Tucker S, Costa-Nunes P, Pontes O, Pikaard CS. Mechanisms of HDA6-mediated rRNA gene silencing: suppression of intergenic Pol II transcription and differential effects on maintenance versus siRNA-directed cytosine methylation. *Genes Dev*. 2010; 24:1119–1132. DOI: 10.1101/gad.1914110 [PubMed: 20516197]
- Exner V, Taranto P, Schonrock N, Gruissem W, Hennig L. Chromatin assembly factor CAF-1 is required for cellular differentiation during plant development. *Dev Camb Engl*. 2006; 133:4163–4172. DOI: 10.1242/dev.02599
- Feng CM, Qiu Y, Van Buskirk EK, Yang EJ, Chen M. Light-regulated gene repositioning in *Arabidopsis*. *Nat Commun*. 2014; 5:3027.doi: 10.1038/ncomms4027
- Filion GJ, van Bommel JG, Braunschweig U, Talhout W, Kind J, Ward LD, Brugman W, de Castro IJ, Kerkhoven RM, Bussemaker HJ, van Steensel B. Systematic protein location mapping reveals five principal chromatin types in *Drosophila* cells. *Cell*. 2010; 143:212–224. DOI: 10.1016/j.cell.2010.09.009 [PubMed: 20888037]
- Flutre T, Duprat E, Feuillet C, Quesneville H. Considering transposable element diversification in de novo annotation approaches. *PLoS One*. 2011; 6:e16526.doi: 10.1371/journal.pone.0016526 [PubMed: 21304975]
- Fransz P, De Jong JH, Lysak M, Castiglione MR, Schubert I. Interphase chromosomes in *Arabidopsis* are organized as well defined chromocenters from which euchromatin loops emanate. *Proc Natl Acad Sci U S A*. 2002; 99:14584–14589. DOI: 10.1073/pnas.212325299 [PubMed: 12384572]
- Gibcus JH, Dekker J. The hierarchy of the 3D genome. *Mol Cell*. 2013; 49:773–782. DOI: 10.1016/j.molcel.2013.02.011 [PubMed: 23473598]
- Graumann K, Evans DE. Nuclear envelope dynamics during plant cell division suggest common mechanisms between kingdoms. *Biochem J*. 2011; 435:661–667. DOI: 10.1042/BJ20101769 [PubMed: 21323637]
- Graumann K, Evans DE. Plant SUN domain proteins: components of putative plant LINC complexes? *Plant Signal Behav*. 2010; 5:154–156. [PubMed: 20023391]
- Grob S, Schmid MW, Luedtke NW, Wicker T, Grossniklaus U. Characterization of chromosomal architecture in *Arabidopsis* by chromosome conformation capture. *Genome Biol*. 2013; 14:R129.doi: 10.1186/gb-2013-14-11-r129 [PubMed: 24267747]
- Grummt I, Langst G. Epigenetic control of RNA polymerase I transcription in mammalian cells. *Biochim Biophys Acta*. 2013; 1829:393–404. DOI: 10.1016/j.bbagr.2012.10.004 [PubMed: 23063748]
- Guelen L, Pagie L, Brasset E, Meuleman W, Faza MB, Talhout W, Eussen BH, de Klein A, Wessels L, de Laat W, van Steensel B. Domain organization of human chromosomes revealed by mapping of nuclear lamina interactions. *Nature*. 2008; 453:948–951. DOI: 10.1038/nature06947 [PubMed: 18463634]

- Guidi M, Ruault M, Marbouty M, Loiodice I, Cournac A, Billaudeau C, Hocher A, Mozziconacci J, Koszul R, Taddei A. Spatial reorganization of telomeres in long-lived quiescent cells. *Genome Biol.* 2015; 16:206.doi: 10.1186/s13059-015-0766-2 [PubMed: 26399229]
- Haeusler RA, Pratt-Hyatt M, Good PD, Gipson TA, Engelke DR. Clustering of yeast tRNA genes is mediated by specific association of condensin with tRNA gene transcription complexes. *Genes Dev.* 2008; 22:2204–2214. DOI: 10.1101/gad.1675908 [PubMed: 18708579]
- Heacock M, Spangler E, Riha K, Puizina J, Shippen DE. Molecular analysis of telomere fusions in *Arabidopsis*: multiple pathways for chromosome end-joining. *EMBO J.* 2004; 23:2304–2313. DOI: 10.1038/sj.emboj.7600236 [PubMed: 15141167]
- Ito H, Kakutani T. Control of transposable elements in *Arabidopsis thaliana*. *Chromosome Res Int J Mol Supramol Evol Asp Chromosome Biol.* 2014; 22:217–223. DOI: 10.1007/s10577-014-9417-9
- Jady BE, Richard P, Bertrand E, Kiss T. Cell cycle-dependent recruitment of telomerase RNA and Cajal bodies to human telomeres. *Mol Biol Cell.* 2006; 17:944–954. DOI: 10.1091/mbc.E05-09-0904 [PubMed: 16319170]
- Kannan K, Nelson ADL, Shippen DE. Dyskerin is a component of the *Arabidopsis* telomerase RNP required for telomere maintenance. *Mol Cell Biol.* 2008; 28:2332–2341. DOI: 10.1128/MCB.01490-07 [PubMed: 18212040]
- Kharchenko PV, Alekseyenko AA, Schwartz YB, Minoda A, Riddle NC, Ernst J, Sabo PJ, Larschan E, Gorchakov AA, Gu T, Linder-Basso D, Plachetka A, Shanower G, Tolstorukov MY, Luquette LJ, Xi R, Jung YL, Park RW, Bishop EP, Canfield TK, Sandstrom R, Thurman RE, MacAlpine DM, Stamatoyannopoulos JA, Kellis M, Elgin SCR, Kuroda MI, Pirrotta V, Karpen GH, Park PJ. Comprehensive analysis of the chromatin landscape in *Drosophila melanogaster*. *Nature.* 2011; 471:480–485. DOI: 10.1038/nature09725 [PubMed: 21179089]
- Kind J, Pagie L, de Vries SS, Nahidiazar L, Dey SS, Bienko M, Zhan Y, Lajoie B, de Graaf CA, Amendola M, Fudenberg G, Imakaev M, Mirny LA, Jalink K, Dekker J, van Oudenaarden A, van Steensel B. Genome-wide Maps of Nuclear Lamina Interactions in Single Human Cells. *Cell.* 2015; 163:134–147. DOI: 10.1016/j.cell.2015.08.040 [PubMed: 26365489]
- Kind J, Pagie L, Ortazokoyun H, Boyle S, de Vries SS, Janssen H, Amendola M, Nolen LD, Bickmore WA, van Steensel B. Single-cell dynamics of genome-nuclear lamina interactions. *Cell.* 2013; 153:178–192. DOI: 10.1016/j.cell.2013.02.028 [PubMed: 23523135]
- Langmead B, Salzberg SL. Fast gapped-read alignment with Bowtie 2. *Nat Methods.* 2012; 9:357–359. DOI: 10.1038/nmeth.1923 [PubMed: 22388286]
- Lee JH, Lee YS, Jeong SA, Khadka P, Roth J, Chung IK. Catalytically active telomerase holoenzyme is assembled in the dense fibrillar component of the nucleolus during S phase. *Histochem Cell Biol.* 2014; 141:137–152. DOI: 10.1007/s00418-013-1166-x [PubMed: 24318571]
- Lermontova I, Schubert V, Bornke F, Macas J, Schubert I. *Arabidopsis* CBF5 interacts with the H/ACA snoRNP assembly factor NAF1. *Plant Mol Biol.* 2007; 65:615–626. DOI: 10.1007/s11103-007-9226-z [PubMed: 17712600]
- McStay B, Grummt I. The epigenetics of rRNA genes: from molecular to chromosome biology. *Annu Rev Cell Dev Biol.* 2008; 24:131–157. DOI: 10.1146/annurev.cellbio.24.110707.175259 [PubMed: 18616426]
- Meister P, Taddei A. Building silent compartments at the nuclear periphery: a recurrent theme. *Curr Opin Genet Dev.* 2013; 23:96–103. DOI: 10.1016/j.gde.2012.12.001 [PubMed: 23312840]
- Mozgova I, Mokros P, Fajkus J. Dysfunction of chromatin assembly factor 1 induces shortening of telomeres and loss of 45S rDNA in *Arabidopsis thaliana*. *Plant Cell.* 2010; 22:2768–2780. DOI: 10.1105/tpc.110.076182 [PubMed: 20699390]
- Nemeth A, Conesa A, Santoyo-Lopez J, Medina I, Montaner D, Peterfia B, Solovei I, Cremer T, Dopazo J, Langst G. Initial genomics of the human nucleolus. *PLoS Genet.* 2010; 6:e1000889.doi: 10.1371/journal.pgen.1000889 [PubMed: 20361057]
- Padeken J, Mendiburo MJ, Chlamydas S, Schwarz HJ, Kremmer E, Heun P. The nucleoplasmin homolog NLP mediates centromere clustering and anchoring to the nucleolus. *Mol Cell.* 2013; 50:236–249. DOI: 10.1016/j.molcel.2013.03.002 [PubMed: 23562326]

- Pecinka A, Schubert V, Meister A, Kreth G, Klatt M, Lysak MA, Fuchs J, Schubert I. Chromosome territory arrangement and homologous pairing in nuclei of *Arabidopsis thaliana* are predominantly random except for NOR-bearing chromosomes. *Chromosoma*. 2004; 113:258–269. DOI: 10.1007/s00412-004-0316-2 [PubMed: 15480725]
- Pederson T. The nucleolus. *Cold Spring Harb Perspect Biol*. 2011; :3.doi: 10.1101/cshperspect.a000638
- Pederson T. The plurifunctional nucleolus. *Nucleic Acids Res*. 1998; 26:3871–3876. [PubMed: 9705492]
- Pontvianne F, Abou-Ellail M, Douet J, Comella P, Matia I, Chandrasekhara C, Debures A, Blevins T, Cooke R, Medina FJ, Tourmente S, Pikaard CS, Saez-Vasquez J. Nucleolin is required for DNA methylation state and the expression of rRNA gene variants in *Arabidopsis thaliana*. *PLoS Genet*. 2010; 6:e1001225.doi: 10.1371/journal.pgen.1001225 [PubMed: 21124873]
- Pontvianne F, Blevins T, Chandrasekhara C, Feng W, Stroud H, Jacobsen SE, Michaels SD, Pikaard CS. Histone methyltransferases regulating rRNA gene dose and dosage control in *Arabidopsis*. *Genes Dev*. 2012; 26:945–957. DOI: 10.1101/gad.182865.111 [PubMed: 22549957]
- Pontvianne F, Blevins T, Chandrasekhara C, Mozgova I, Hassel C, Pontes OMF, Tucker S, Mokros P, Muchova V, Fajkus J, Pikaard CS. Subnuclear partitioning of rRNA genes between the nucleolus and nucleoplasm reflects alternative epiallelic states. *Genes Dev*. 2013; 27:1545–1550. DOI: 10.1101/gad.221648.113 [PubMed: 23873938]
- Pontvianne F, Matia I, Douet J, Tourmente S, Medina FJ, Echeverria M, Saez-Vasquez J. Characterization of AtNUC-L1 reveals a central role of nucleolin in nucleolus organization and silencing of AtNUC-L2 gene in *Arabidopsis*. *Mol Biol Cell*. 2007; 18:369–379. DOI: 10.1091/mbc.E06-08-0751 [PubMed: 17108323]
- Pratt-Hyatt M, Pai DA, Haeusler RA, Wozniak GG, Good PD, Miller EL, McLeod IX, Yates JR 3rd, Hopper AK, Engelke DR. Mod5 protein binds to tRNA gene complexes and affects local transcriptional silencing. *Proc Natl Acad Sci U S A*. 2013; 110:E3081–3089. DOI: 10.1073/pnas.1219946110 [PubMed: 23898186]
- Roberts NY, Osman K, Armstrong SJ. Telomere distribution and dynamics in somatic and meiotic nuclei of *Arabidopsis thaliana*. *Cytogenet Genome Res*. 2009; 124:193–201. DOI: 10.1159/000218125 [PubMed: 19556773]
- Roudier F, Ahmed I, Berard C, Sarazin A, Mary-Huard T, Cortijo S, Bouyer D, Caillieux E, Duvernois-Berthet E, Al-Shikhley L, Giraut L, Despres B, Drevensek S, Barneche F, Derozier S, Brunaud V, Aubourg S, Schnittger A, Bowler C, Martin-Magniette ML, Robin S, Caboche M, Colot V. Integrative epigenomic mapping defines four main chromatin states in *Arabidopsis*. *EMBO J*. 2011; 30:1928–1938. DOI: 10.1038/emboj.2011.103 [PubMed: 21487388]
- Roy S, Ernst J, Kharchenko PV, Kheradpour P, Negre N, Eaton ML, Landolin JM, Bristow CA, Ma L, Lin MF, Washietl S, Arshinoff BI, Ay F, Meyer PE, Robine N, Washington NL, Di Stefano L, Berezikov E, Brown CD, Candeias R, Carlson JW, Carr A, Jungreis I, Marbach D, Sealfon R, Tolstorukov MY, Will S, Alekseyenko AA, Artieri C, Booth BW, Brooks AN, Dai Q, Davis CA, Duff MO, Feng X, Gorchakov AA, Gu T, Henikoff JG, Kapranov P, Li R, MacAlpine HK, Malone J, Minoda A, Nordman J, Okamura K, Perry M, Powell SK, Riddle NC, Sakai A, Samsonova A, Sandler JE, Schwartz YB, Sher N, Spokony R, Sturgill D, van Baren M, Wan KH, Yang L, Yu C, Feingold E, Good P, Guyer M, Lowdon R, Ahmad K, Andrews J, Berger B, Brenner SE, Brent MR, Cherbas L, Elgin SCR, Gingeras TR, Grossman R, Hoskins RA, Kaufman TC, Kent W, Kuroda MI, Orr-Weaver T, Perrimon N, Pirrotta V, Posakony JW, Ren B, Russell S, Cherbas P, Graveley BR, Lewis S, Micklem G, Oliver B, Park PJ, Celniker SE, Henikoff S, Karpen GH, Lai EC, MacAlpine DM, Stein LD, White KP, Kellis M. Identification of functional elements and regulatory circuits by *Drosophila* modENCODE. *Science*. 2010; 330:1787–1797. DOI: 10.1126/science.1198374 [PubMed: 21177974]
- Ruckova E, Friml J, Prochazkova Schrupfova P, Fajkus J. Role of alternative telomere lengthening unmasked in telomerase knock-out mutant plants. *Plant Mol Biol*. 2008; 66:637–646. DOI: 10.1007/s11103-008-9295-7 [PubMed: 18239859]
- Schubert V, Berr A, Meister A. Interphase chromatin organisation in *Arabidopsis* nuclei: constraints versus randomness. *Chromosoma*. 2012; 121:369–387. DOI: 10.1007/s00412-012-0367-8 [PubMed: 22476443]



- Schubert V, Rudnik R, Schubert I. Chromatin associations in Arabidopsis interphase nuclei. *Front Genet.* 2014; 5:389.doi: 10.3389/fgene.2014.00389 [PubMed: 25431580]
- Schubert V, Weisshart K. Abundance and distribution of RNA polymerase II in Arabidopsis interphase nuclei. *J Exp Bot.* 2015; 66:1687–1698. DOI: 10.1093/jxb/erv091 [PubMed: 25740920]
- Sequeira-Mendes J, Araguez I, Peiro R, Mendez-Giraldez R, Zhang X, Jacobsen SE, Bastolla U, Gutierrez C. The Functional Topography of the Arabidopsis Genome Is Organized in a Reduced Number of Linear Motifs of Chromatin States. *Plant Cell.* 2014; 26:2351–2366. DOI: 10.1105/tpc.114.124578 [PubMed: 24934173]
- Sequeira-Mendes J, Gutierrez C. Genome architecture: from linear organisation of chromatin to the 3D assembly in the nucleus. *Chromosoma.* 2015; doi: 10.1007/s00412-015-0538-5
- Stepinski D. Functional ultrastructure of the plant nucleolus. *Protoplasma.* 2014; 251:1285–1306. DOI: 10.1007/s00709-014-0648-6 [PubMed: 24756369]
- Tatout C, Evans DE, Vanrobays E, Probst AV, Graumann K. The plant LINC complex at the nuclear envelope. *Chromosome Res Int J Mol Supramol Evol Asp Chromosome Biol.* 2014; 22:241–252. DOI: 10.1007/s10577-014-9419-7
- Thiry M, Lafontaine DLJ. Birth of a nucleolus: the evolution of nucleolar compartments. *Trends Cell Biol.* 2005; 15:194–199. DOI: 10.1016/j.tcb.2005.02.007 [PubMed: 15817375]
- Thompson M, Haeusler RA, Good PD, Engelke DR. Nucleolar clustering of dispersed tRNA genes. *Science.* 2003; 302:1399–1401. DOI: 10.1126/science.1089814 [PubMed: 14631041]
- Tomlinson RL, Ziegler TD, Supakorndej T, Terns RM, Terns MP. Cell cycle- regulated trafficking of human telomerase to telomeres. *Mol Biol Cell.* 2006; 17:955–965. DOI: 10.1091/mbc.E05-09-0903 [PubMed: 16339074]
- Tucker S, Vitins A, Pikaard CS. Nucleolar dominance and ribosomal RNA gene silencing. *Curr Opin Cell Biol.* 2010; 22:351–356. DOI: 10.1016/j.jceb.2010.03.009 [PubMed: 20392622]
- van Koningsbruggen S, Gierlinski M, Schofield P, Martin D, Barton GJ, Ariyurek Y, den Dunnen JT, Lamond AI. High-resolution whole-genome sequencing reveals that specific chromatin domains from most human chromosomes associate with nucleoli. *Mol Biol Cell.* 2010; 21:3735–3748. DOI: 10.1091/mbc.E10-06-0508 [PubMed: 20826608]
- Vespa L, Warrington RT, Mokros P, Siroky J, Shippen DE. ATM regulates the length of individual telomere tracts in Arabidopsis. *Proc Natl Acad Sci U S A.* 2007; 104:18145–18150. DOI: 10.1073/pnas.0704466104 [PubMed: 17989233]
- Wang L, Haeusler RA, Good PD, Thompson M, Nagar S, Engelke DR. Silencing near tRNA genes requires nucleolar localization. *J Biol Chem.* 2005; 280:8637–8639. DOI: 10.1074/jbc.C500017200 [PubMed: 15654076]
- Wang Z, Zang C, Rosenfeld JA, Schones DE, Barski A, Cuddapah S, Cui K, Roh TY, Peng W, Zhang MQ, Zhao K. Combinatorial patterns of histone acetylations and methylations in the human genome. *Nat Genet.* 2008; 40:897–903. DOI: 10.1038/ng.154 [PubMed: 18552846]

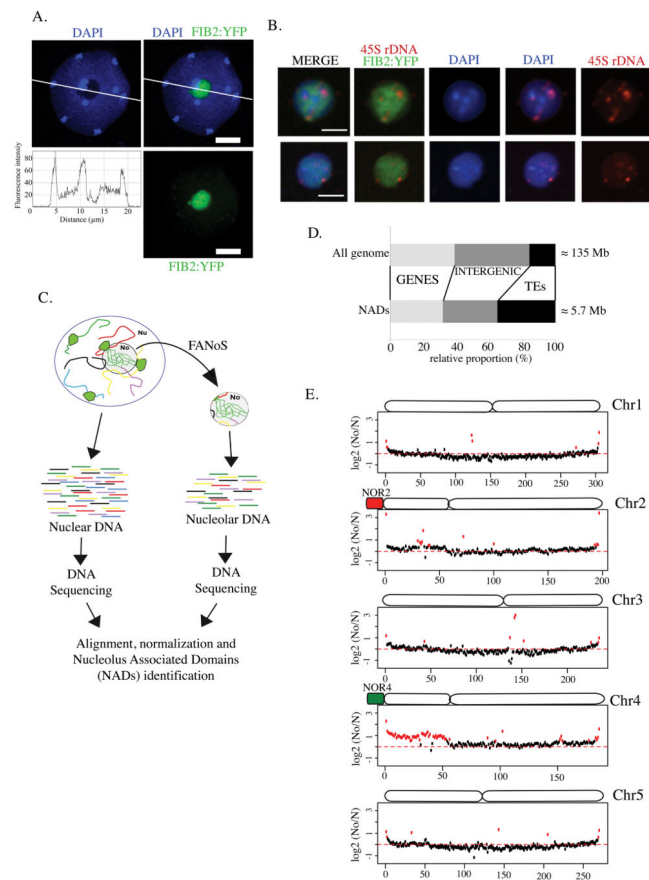


**Figure 1. Identification of nucleolus-associated chromatin domains (NADs) in *A. thaliana***

**A.** One z-stack of a DAPI-stained (blue) nucleus from an *A. thaliana* leaf expressing the Fib2:YFP (green) marker. The white line segment indicates positions traversing the nucleus where DAPI signal intensity was plotted as a function of distance along the segment (profile below). Scale bar is 5 µm. **B.** Confocal images of two FACS-isolated nucleoli where DNA is stained by DAPI (blue), the Fib2:YFP marker delimits the nucleolus (green) and rRNA genes are detected by DNA-FISH (rDNA, red). Scale bar is 2 µm. **C.** Cartoon depicting the strategy used to isolate and sequence total nuclear (N) and specifically nucleolar (No) DNA in order to identify NADs by deep sequencing. **D.** Bar plot displaying the proportion of different types of sequence in NADs (below) relative to the entire genome (above). **E.** Chromosome plots displaying the relative enrichment of a given genomic segment in the nucleolus of wild-type Col-0. The y-axis displays the fold change ratio No/N. Each dot represents a 100kb window. Nucleolus-enriched genomic regions above the threshold (red-dotted line) are coloured in red.

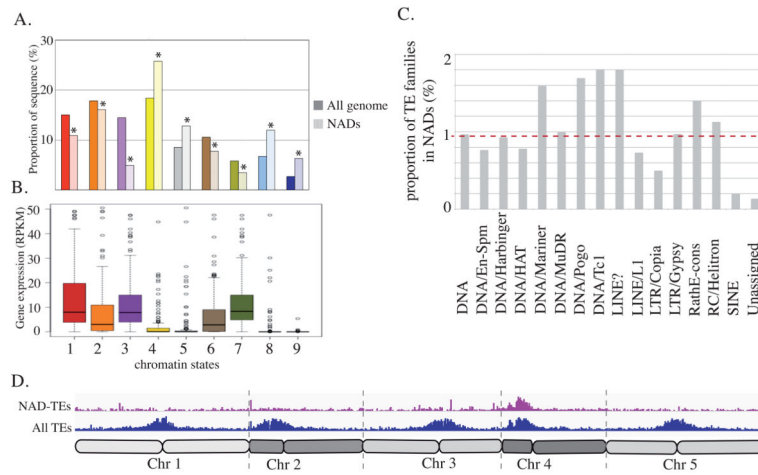


**Figure 2. Epigenetic characteristics of NADs**

A. Histogram representing the relative enrichment of each chromatin state in NADs compared to the entire reference genome. B. Box plot representing the relative expression of NAD-genes present in each category of chromatin state. C. Histogram displaying the relative proportions of each TE superfamily in NADs. The red-dotted line represents the 1X expected enrichment. D. Distribution of all TEs (blue) and NAD-TEs (violet) along all 5 chromosomes.

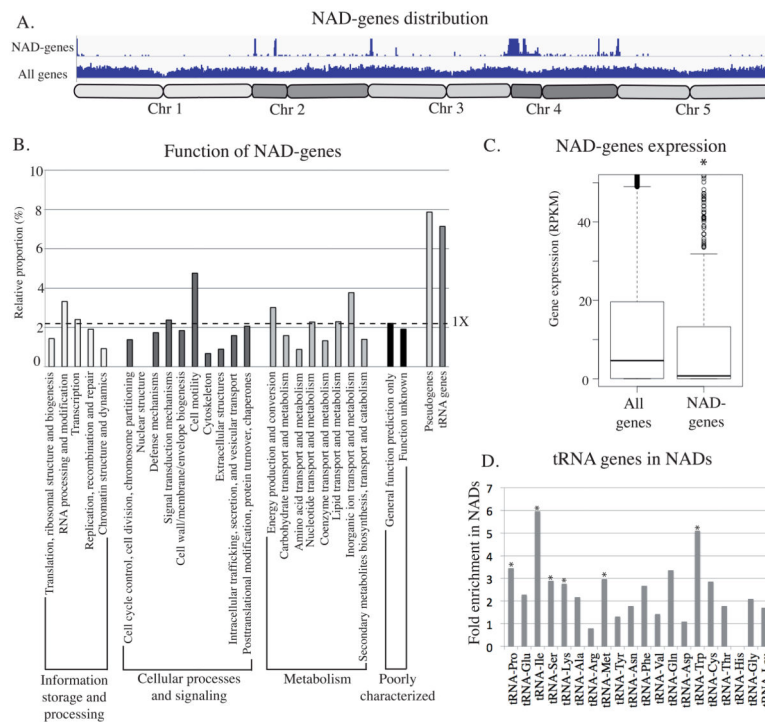


**Figure 3. Description of NAD-gene**

A. Distribution of all genes and NAD-genes along all 5 chromosomes. B. Histogram displaying the relative enrichment of NAD-genes in each cluster of orthologous groups (COGs), among pseudogenes and tRNA-genes. The dotted line represents the 1X expected enrichment. C. Dot-plot revealing the relative expression of all genes or NAD-genes in 3 week-old leaves. D. Histogram displaying the relative enrichment of each class of tRNA genes in NADs. The asterisk is present when the enrichment is statistically demonstrated.

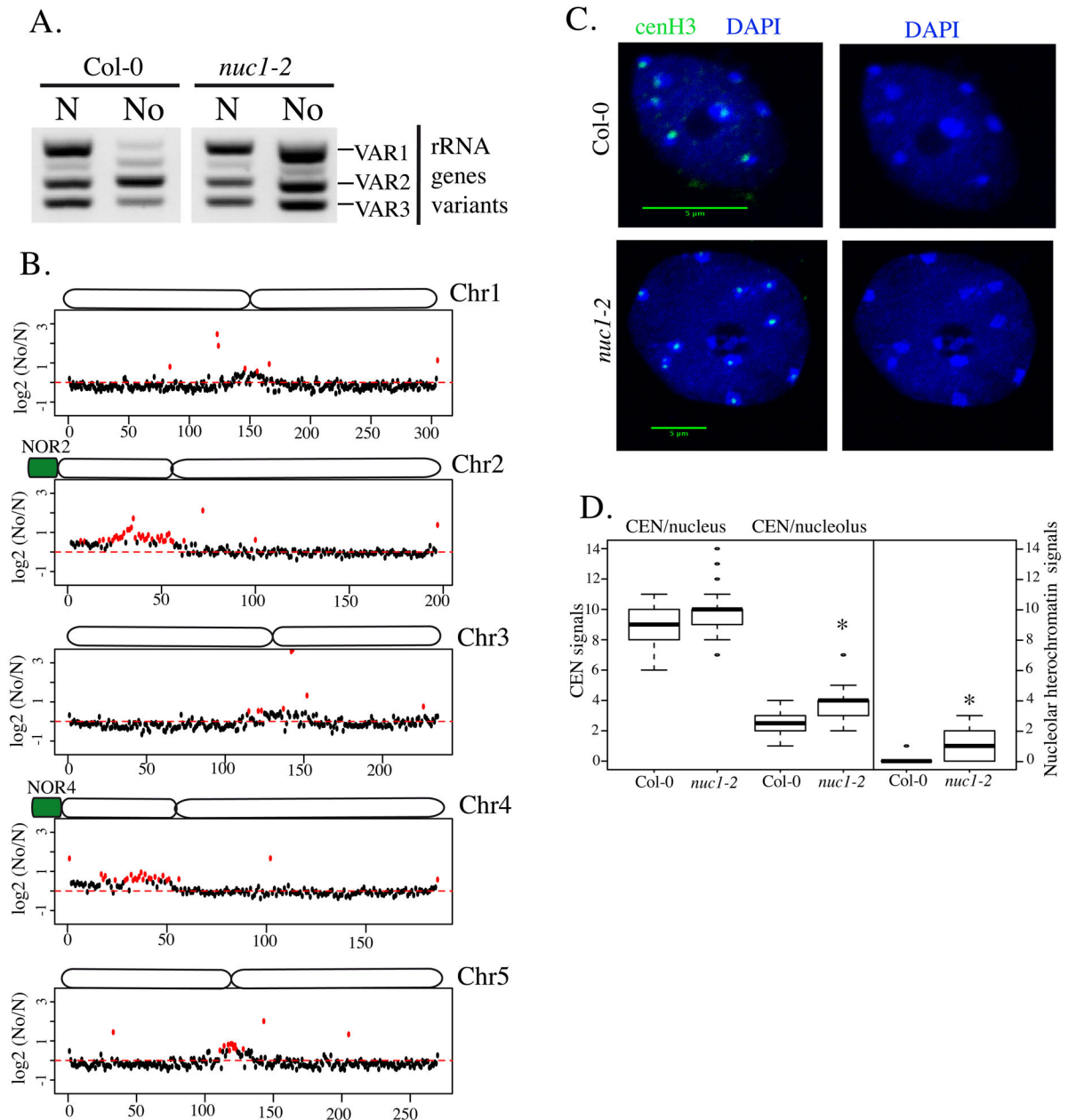


**Figure 4. Identification of NADs in *nuc1* mutant**

A. PCR detection of rRNA gene variant types in DNA of purified nuclei (N) or nucleoli (No) of wild-type (Col-0) or *nuc1* plants. B. Chromosome plots displaying the relative enrichment of genomic sequence as 100kb windows in the nucleolus on each 5 chromosomes in *nuc1* mutant. C. DAPI-stained nuclei from WT Col-0 (left panel) or from *nuc1* plants (right panel). The green signal represent the fluorescence obtained from the anti-cenH3 antibody. Scale bar is 5μm. D. Box-plot showing the relative proportion of nucleolus-associated centromeres in WT Col-0 or in *nuc1* mutant. The analysis was performed on 100 nuclei per samples. F. Box-plot displaying the relative number of heterochromatic signals inside the

nucleolus in WT Col-0 or in *nuc1* mutant. The asterisk is present when the enrichment is statistically demonstrated.

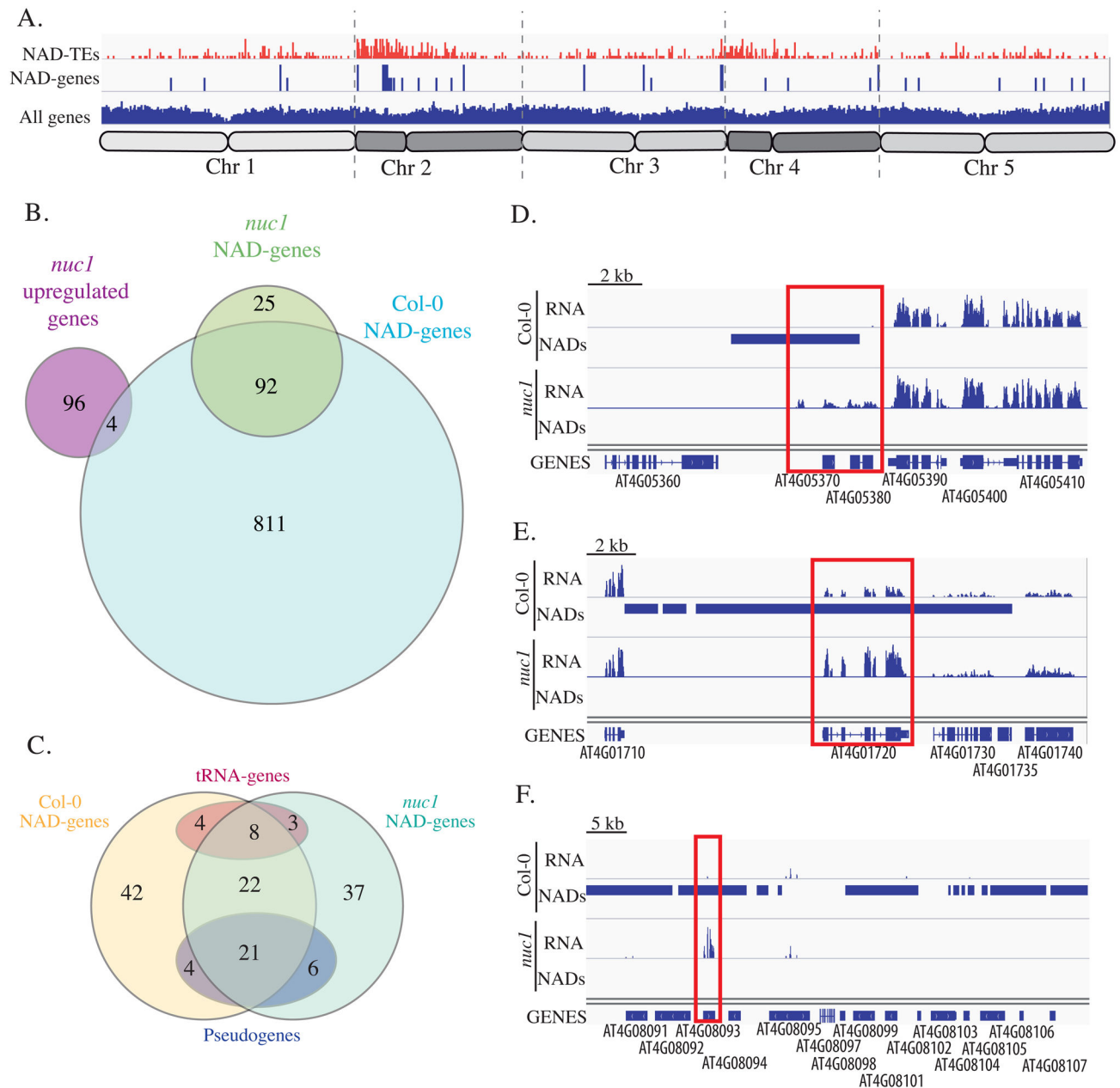


**Figure 5. Comparison of NAD-genes in wild-type versus *nuc1* mutant**

A. Distribution of all genes, NAD-TEs (red) and NAD-genes (blue) in *nuc1* mutant along all 5 chromosomes. B. Venn diagram showing the relation between NAD-genes from wild-type Col-0 and the *nuc1* mutant, as well as the genes up-regulated in *nuc1* mutant. C. Venn diagram displaying common features between NAD-genes highly associating with the nucleolus in wild-type versus *nuc1* mutant. D–F. Genome browser screenshot showing three examples of NAD-genes in Col-0 whom nucleolus association is lost in *nuc1* and is accompanied by a significant increase of their expression.

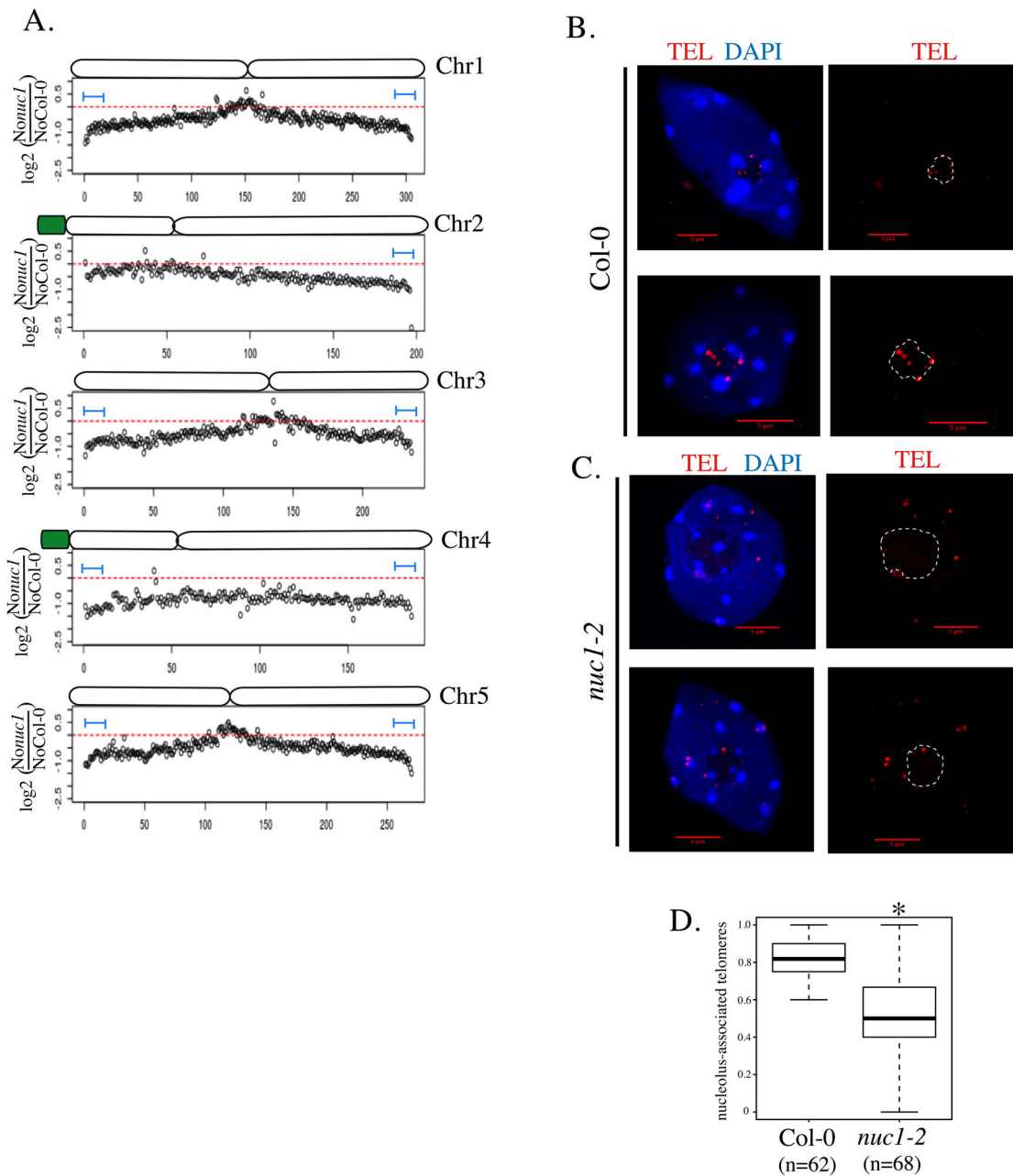


**Figure 6. Telomere nucleolar clustering is affected in *nucl1* mutant**

A. Chromosome-plot displaying the relative enrichment of genomic sequence as 100kb windows in the nucleolus on each 5 chromosomes of *nucl1* mutant versus WT Col-0. B–C. DNA-FISH analyses using a telomere specific probe (red signal) on DAPI-stained nuclei (Blue) from WT Col-0 (B) or from *nucl1* plants (C). D. Box-plot showing the proportion of nucleolus-associated telomeres in WT Col-0 (from 62 nuclei) and in *nucl1* mutant (from 68 nuclei). The asterisk is present when the enrichment is statistically demonstrated.



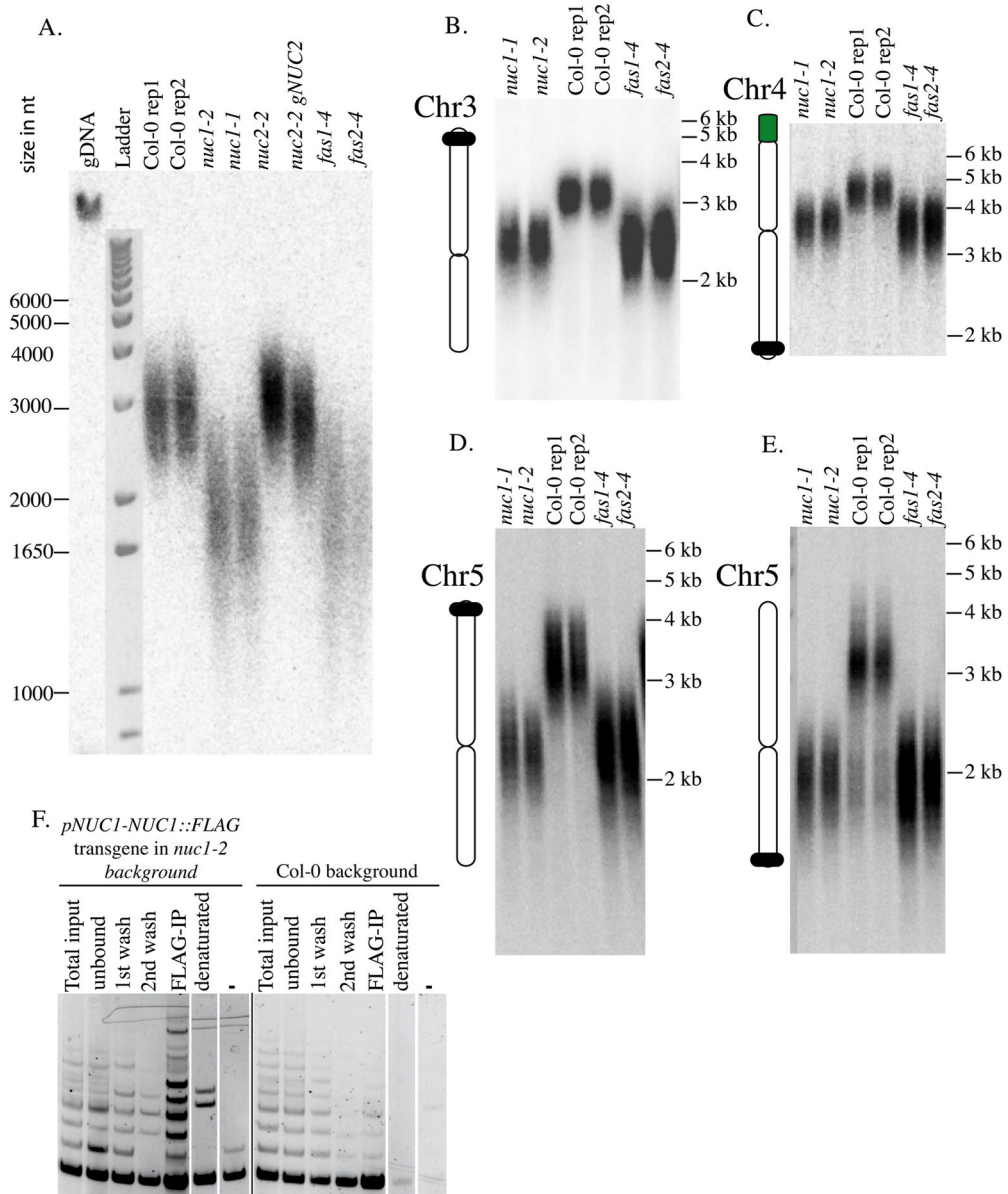


**Figure 7. NUC1 interacts with Telomerase and its disruption induces telomeres shortening**  
 A. TRF analyses of telomere length in 2 WT Col-0 replicates, 2 *nuc1* mutant alleles, *nuc2-2* or complemented *nuc2* mutant, as well as in *fas1-4* and *fas2-4* mutant. B–E. PETRA analyses of telomere length in 2 *nuc1* mutant alleles, 2 replicates of WT Col-0, as well as in *fas1-4* and *fas2-4* mutants. Chromosome specific probes were used to detect the telomere of the left arm of chromosome 3 (B), the right arm of chromosome 4 (C), as well as the left (D) or right (E) arm of chromosome 5. (F) Telomerase activity was analyzed in fractions obtained during the IP-TRAP experiment using pNUC1-NUC1-FLAG-tagged and WT Col-0 plants. Total input, total protein extract prior to IP; unbound, unbound fraction after the capture by ANTI-FLAG magnetic beads; 1st wash, 1st wash of the fraction bound to magnetic beads with buffer W; 2nd wash, 2nd wash of the fraction bound to magnetic beads

with buffer W; FLAG-IP, a fraction specifically bound to magnetic beads; denatured, reaction with denatured total protein extract (5 min, 95 °C); -, reaction with buffer W.